

Fourth family neutrinos and the Higgs boson at the LHC

T. Çuhadar-Dönszelmann,^a M. Karagöz Ünel,^b V.E. Özcan,^c S. Sultansoy^{de} and G. Ünel^{fg}

^aUniversity of Sheffield, Department of Physics and Astronomy,
Hounsfield Road, Sheffield, S3 7RH, U.K.

^bDepartment of Physics, University of Oxford,
Oxford, OX1 3RH, U.K.

^cDepartment of Physics and Astronomy, University College London,
Gower St., London, WC1E 6BT, U.K.

^dPhysics Department, TOBB University of Economics and Technology,
Sogutozu Cad 43, Ankara, Turkey

^eInstitute of Physics, Academy of Sciences,
H. Cavid Avenue 143, Baku, Azerbaijan

^fPhysics Department, CERN, CH-1211 Geneva 23, Switzerland

^gDepartment of Physics and Astronomy, University of California at Irvine,
Irvine, CA 92697, U.S.A.

E-mail: tulay.cuhadar.donszelmann@cern.ch, muge.karagoz.unel@cern.ch,
eo@hep.ucl.ac.uk, ssultansoy@etu.edu.tr, gokhan.unel@cern.ch

ABSTRACT: We evaluate the LHC discovery potential for the fourth family Standard Model neutrinos in the process $pp \rightarrow Z/h \rightarrow \nu_4 \bar{\nu}_4 \rightarrow W\mu W\mu$. We show that, depending on their masses, the simultaneous discovery of both the Higgs boson and the heavy neutrinos is probable at early stages of LHC operation. Results are presented for both Majorana and Dirac type fourth family neutrinos.

KEYWORDS: Beyond Standard Model, Standard Model.

Contents

1. Introduction	1
2. Fourth family neutrinos at the LHC	2
2.1 Impact of fourth family quarks on Higgs boson production	2
2.2 Heavy neutrino discovery channels	3
3. Analysis strategy	5
3.1 Signal properties	6
3.2 Background processes	6
3.3 Event selection and reconstruction	7
3.4 Dirac vs Majorana neutrinos	8
3.4.1 Majorana case	9
3.4.2 Dirac case	9
4. Results and discussion	10
5. Conclusions	11

1. Introduction

The main goal of the LHC experiments is the vindication or rejection of the Higgs mechanism as the underlying cause of fermion masses in the Standard Model (SM). Higgs boson searches are therefore of utmost importance. Understanding the flavor structure of the SM, including the determination of the number of fermion families, is also a key goal. The data from LEP-1 strongly favored three families of fermions with light neutrinos ($m_\nu < m_Z/2$) [1]. Thus, there are no experimental or phenomenological evidence excluding the existence of a fourth fermion family with a heavy neutrino. Indeed, the recent electroweak precision data are equally consistent with the presence of three or four fermion families [2, 3], whereas the four family scenario is favored if the Higgs is heavier than 200 GeV [4]. These compelling reasons form a primary argument to search for a fourth SM family with heavy fermions. A secondary impetus arises from the as yet unexplained hierarchy observed in fermion masses. If there were four SM families and their Yukawa couplings were identical, then the diagonalization of the 4×4 mass matrix in which all elements are unity, would yield a single non-zero element (M_{44}) [5–7]. In this case, the observed masses of fermions in the first three families can be obtained from perturbations on uniform 4×4 mass matrices [8–10]. This idea is referred to in the literature as “flavour democracy”: see the review in [11] and references therein. A third and more recent motivation for the fourth family arises from the proposed charge-spin unification [12]. Finally,

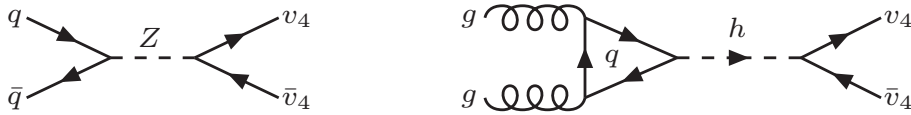


Figure 1: Possible ν_4 pair production via Z (left) or Higgs boson (right) at the LHC.

recent measurements from the B factories and the Tevatron have shown deviations from the SM, which have been attributed to the possible existence of a fourth generation [13–15].

From an experimentalist’s point of view, a heavy quark and a heavy neutrino are both very interesting particles to search for at the LHC. Searches for heavy quarks of the fourth SM family have been considered elsewhere [16–19]. Heavy neutrinos can be produced in pairs at the LHC and are expected to decay to a W boson and a charged lepton with flavor dependent on the particular Maki-Nakagawa-Sakata (MNS) matrix [10]. The Majorana or Dirac nature of the fermions will have an important impact on the observed outcome: those final states, in which both leptons have the same sign, are expected to be free of direct backgrounds and therefore offer a distinct signature. The use of such signatures for Higgs boson discovery via a so-called “silver mode” was recently proposed [20]. While inclusive final states with single fourth family members might be enhanced by lower production-energy threshold, their production cross-sections have a sine-squared dependence on mixing angle and thus, are heavily suppressed.

In this paper, the impact of fourth family quarks on the Higgs boson production and subsequent decay of the Higgs boson into fourth family neutrinos are considered in detail. The Z boson mediated production of the heavy neutrinos and their decay are also studied for Higgsless scenarios.

2. Fourth family neutrinos at the LHC

The 3-family SM is extended with an additional set of quarks and leptons denoted as: u_4 and d_4 for quarks, e_4 for the charged lepton and ν_4 for the heavy neutrino. The fermion-boson interaction vertices of the fourth family fermions are similar to the first three families. Although the masses and the mixings of the new fermions are not fixed, the lower bound on the mass of the fourth family quarks from Tevatron experiments is 250 GeV [21]. Following the flavour democracy approach, the masses of u_4 and d_4 are taken to be degenerate and represented as m_{q_4} .

The tree-level diagrams for the pair production of the fourth SM family heavy neutrinos are shown in figure 1. The pair production cross section of the virtual Z boson mediated channel depends on the mass of the ν_4 while that of Higgs mediated channel depends on the Higgs and ν_4 masses as well as the q_4 mass, which contributes to the quark loop in figure 1.

2.1 Impact of fourth family quarks on Higgs boson production

The enhancement of the Higgs production cross section at the LHC due to the fourth

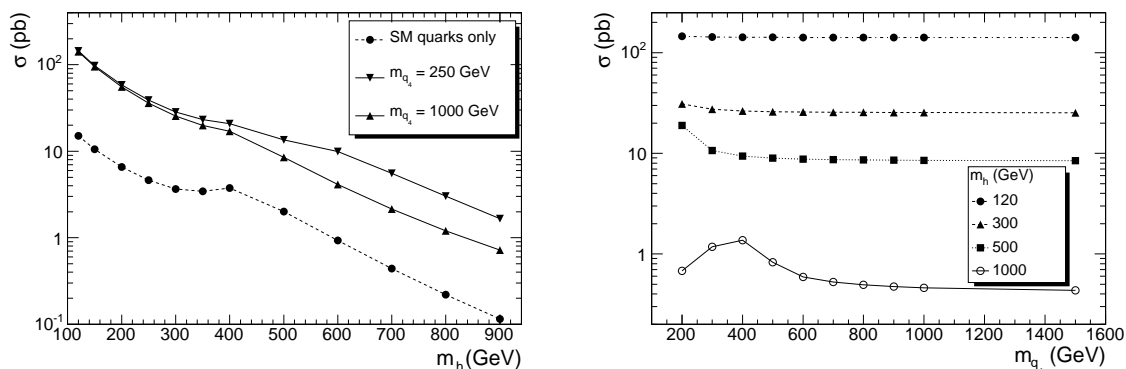


Figure 2: Higgs boson production cross section as a function of Higgs mass, for SM (circles), SM + fourth family for $m_{q_4} = 1000$ GeV (upwards triangles) and similarly for $m_{q_4} = 250$ GeV (downwards triangles) (left). Higgs boson production cross section as a function of the new quark mass, for different Higgs boson mass values: 120, 300, 500 and 1000 GeV (right).

family quarks via the gluon loop was previously calculated with the infinite mass quark approximation [22]. For a more realistic cross section calculation, we modified the Higgs production cross section software, `Higlu` [23], to include the effects of the fourth family quarks with definite masses. On the left-hand side of figure 2, the Higgs production cross section of 3-family SM is compared with that of 4-family SM, for $m_{q_4} = 250$ GeV and $m_{q_4} = 1000$ GeV. It is seen that, by comparison to the results in [22], $m_{q_4} = 1000$ GeV is a good approximation to the infinite mass approximation. To further investigate the validity of this approximation, the same cross section is also plotted in figure 2 (right), as a function of the fourth family quark mass (m_{q_4}) for Higgs boson mass values of 120, 300, 500 and 1000 GeV. It is seen that for a Higgs boson of $m_h \leq 300$ GeV the production cross section is independent of the m_{q_4} , however for $m_h \geq 500$ GeV, the deviation in the cross section is substantial if $m_{q_4} = 400$ GeV. Therefore, for the rest of this note, for the Higgs production cross section values, we use the leading order (LO) results obtained with `Higlu` in the presence of a fourth family with $m_{q_4} = 500$ GeV.

2.2 Heavy neutrino discovery channels

The Higgs boson branching fractions (Br) in the presence of the fourth SM family depend on their masses. Figure 3 shows the Higgs branching fraction to the fourth family neutrinos in the m_h vs m_{ν_4} plane with $m_{q_4} = m_{e_4} = 500$ GeV. It is observed that the highest $Br(h \rightarrow \nu_4 \bar{\nu}_4) = 10\%$ is obtained for the values of $m_h = 250$ GeV and $m_{\nu_4} = 90$ GeV. The branching fractions of the Higgs boson decaying into its main channels such as W^+W^- , ZZ , $t\bar{t}$ are presented in figure 4 as a function of the ν_4 mass, for $m_h = 300$ GeV and $m_h = 500$ GeV. The width of the Higgs boson at these two mass values is around 9 and 67 GeV respectively.

In the absence of the Higgs boson, the virtual Z boson mediated channel will, in fact, be the only ν_4 pair production mechanism. The cross section of the ν_4 pair production is calculated for three cases: Higgsless scenario (i.e. the Z-boson channel), Higgs with

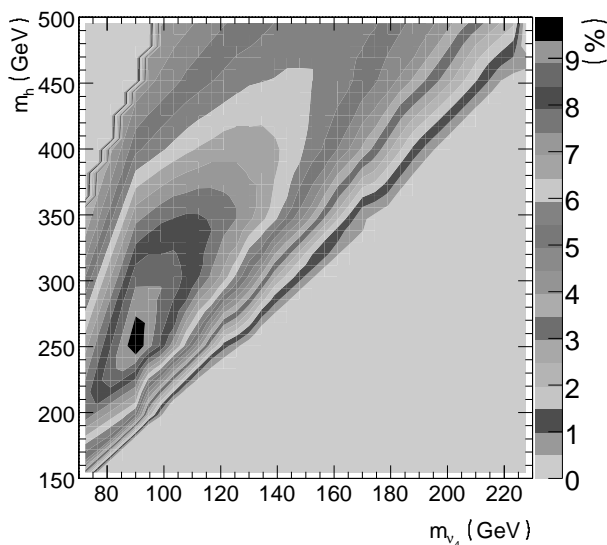


Figure 3: Branching fraction of the Higgs boson decaying into ν_4 pairs in the 2D plane of Higgs and ν_4 masses.

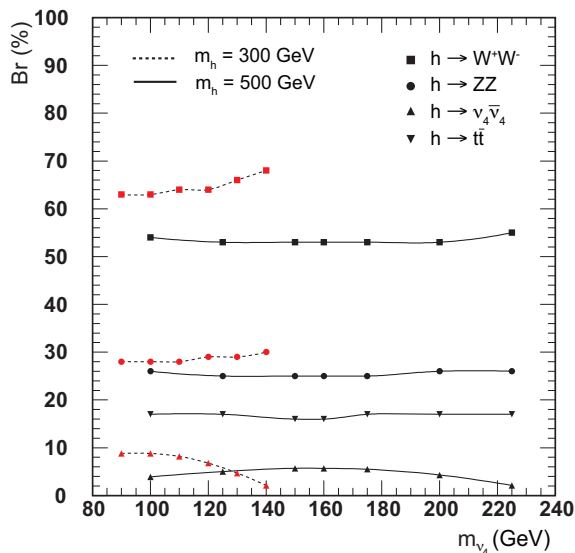


Figure 4: Branching fractions of the Higgs boson decaying into W, Z, ν_4 or top-quark pairs, in the presence of a fourth family with $m_{q_4} = m_{e_4} = 500\text{GeV}$. The dashed (solid) line corresponds to the branching fraction at $m_h = 300(500)$ GeV.

mass $m_h = 300\text{ GeV}$ and $m_h = 500\text{ GeV}$.¹ The results of this calculation, as a function of ν_4 mass are shown in figure 5. For the detailed study of implications at the LHC, one benchmark point for each case is selected, hereafter represented by $S1$, $S2$ and $S3$. The properties of these benchmark points and corresponding effective cross sections are given

¹Electroweak precision data, in the presence of some new physics, favors high masses for the Higgs boson [24].

	$\sigma_{pp \rightarrow Z \rightarrow \nu_4 \bar{\nu}_4}$ (fb)	m_h (GeV)	$\sigma_{gg \rightarrow h}$ (pb)	m_{ν_4} (GeV)	$\text{BR}(h \rightarrow \nu_4 \bar{\nu}_4)$	$\sigma_{pp \rightarrow \nu_4 \bar{\nu}_4 \rightarrow WW \mu \mu}$ (fb)
$S1$	782	N/A	N/A	100	N/A	362
$S2$	782	300	30	100	0.088	1583
$S3$	144	500	10	160	0.055	321

Table 1: Benchmark points for the ν_4 discovery with $m_{q_4} = 500$ GeV. $S1$ point is for the Z boson mediated case, $S2$ $m_h = 300$ GeV, $S3$ $m_h = 500$ GeV. The cross sections of $S2$ and $S3$ include the contribution from the Z boson.

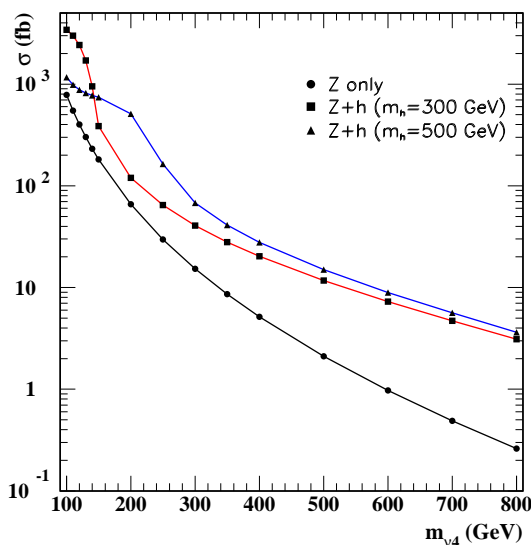


Figure 5: $\nu_4 \bar{\nu}_4$ pair production cross section as a function of ν_4 mass for three scenarios: Higgsless case and cases with $Z+h$ ($m_h = 300$ GeV and $m_h = 500$ GeV). The enhancement from gluon fusion is calculated for $q_4 = u_4, d_4$ mass of 500 GeV.

in table 1 for $m_{q_4}=500$ GeV. The effective cross sections in the last column of table 1, with $WW\mu\mu$ final state, are calculated using the branching fractions given in [10]. In that study, the four-dimensional CKM matrix has been parameterized as a modification of 4×4 unit matrix, and the values for the three degrees of freedom in this parameterization have been extracted from the available experimental data. The parameterization is common between the quark and lepton sectors and predicts $Br(\nu_4 \rightarrow W\mu) = 0.68$ for different values of the assumed unified Yukawa coupling coefficient and the corresponding values of the aforementioned parameters.

It is worth noting that a similar study of Higgs-mediated production of heavy neutrinos was performed for the Superconducting Super Collider, but with significantly less emphasis on the background estimations [25].

3. Analysis strategy

The final experimental signature depends on the nature of ν_4 . If ν_4 is of Majorana type,

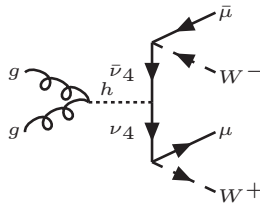


Figure 6: Feynman diagram for the ggh effective coupling vertex also showing final states with W and μ .

the decay products would be two same-sign (SS) leptons and bosons half of the time and opposite-sign (OS) leptons and bosons for the rest of the time. The case with SS leptons has no direct SM model processes to contribute to its background. If ν_4 is a Dirac particle, the signature will be with two OS leptons all the time. In brief, either same-sign or opposite-sign high p_T dileptons are produced in association with two W bosons. The leptons in the event can be used for triggering. The W bosons can be reconstructed from their hadronic decays and/or using leptonic decay of one W boson to reduce the combinatoric background due to high jet multiplicity. A full reconstruction of an event make the measurement of the mass and the width of the both Higgs boson and ν_4 possible. In this paper, only the hadronic decay channels of both W bosons (thus their reconstruction) are considered.

3.1 Signal properties

A tree level signal generator, **CompHEP** 4.4.3 has been used to implement the 4-family SM [26]. We have implemented the loop level process $gg \rightarrow h$ through an effective ggh vertex coupling into **CompHEP**. The coupling strength was adjusted to match the LO **Higlu** results. The production of the Higgs boson via the ggh vertex and its decay via the fourth family neutrinos is shown in figure 6 for OS final states.

We have generated signal events using **CompHEP** and background events using **MadGraph** 4.2.0 [27]. The compatibility between these two tree-level Monte Carlo generators has been previously discussed [28]. The generated events are further processed in **PYTHIA** 6.4.14 [29] for hadronization, addition of multiple interactions and underlying event as well as initial and final state radiation. Finally, a fast simulation of the detector effects, such as acceptance and resolution, is performed with **PGS** [31] using the parameterization for the ATLAS detector [16].²

3.2 Background processes

The main background to ν_4 pair production is massive diboson associated dimuon production: $2V + 2\mu$ where $V = W, Z$. In the case of a Majorana ν_4 , there are no direct SM model processes to contribute to the background, making this channel experimentally appealing. In the case of a Dirac ν_4 , we calculated the total direct SM backgrounds in $2\mu + 2V$ state with **MadGraph** where the renormalization and regularization scale was set to the mass

²Since PGS does not simulate any muon mischarge, this feature was manually added with the mischarge rate parameterized as a function of the muon transverse momentum ($\epsilon_{\text{mischarge}} = 10^{-4+P_T/200\text{GeV}}$) [32].

of the Z boson and CTEQ6L1 was selected as the PDF set [33]. The breakdown of the most dominant SM background processes and their cross sections can be found in table 2 left side. A minimum p_T requirement of 15 GeV was imposed at the generator level in **MadGraph**. It is evident from the table that the direct SM backgrounds even for the Dirac case are essentially negligible. The most generic formulation of the background processes is in fact $2\mu 4j$ final state. However, the computational power at hand was not sufficient to compute the cross section and generate events with **MadGraph**. Since the main contribution to the $2\mu 4j$ final state would come from $\gamma/Z + 4j$ events, a dedicated software, **AlpGen** 2.1.3 [30] was used to calculate their tree-level cross section. With the previously mentioned generator level selection criteria, the cross section is found to be 56.7 ± 0.4 pb. For the event generation, a shorter conservative alternative method is applied:³ all processes yielding the $\gamma/ZWjj$ final states⁴ are studied with **MadGraph** to calculate the cross section (as listed in table 2 right side) and to generate events which are then scaled up to the full cross section obtained from **AlpGen** (same table, last line). The conservativeness of the approach comes from the fact that, in the worst case scenario, the jets in the final state would truly come from the decay of a W boson, otherwise from an underlying event or from QCD radiation. The last two are easier to eliminate by reconstructing the W boson invariant mass. Therefore the sole consideration of the W bosons, as the source of the jets in the final state, is a conservative approach. These events are considered as direct background for the rest of this note.

For the indirect SM background, we consider the $t\bar{t}$ pair production as the overwhelming candidate with a total cross section of 754.7 ± 1.0 pb, calculated with **MadGraph**. The top quark pair production will produce a $2W + 2b_j$ final state, which makes it a candidate for indirect background through misidentification and additional false jet combinatorics for the W boson reconstruction. A possible way for such a case to fake the signal final state would be to have W bosons decay leptonically with small neutrino energy in the presence of additional jet activity (e.g. initial or final state radiation). If both bosons decay leptonically with small neutrino energy then the combination of a high energy lepton and a light jet or a b -jet can mimic the signal. Therefore the $t\bar{t}$ pair production is considered as the indirect background for the remainder of this note.

3.3 Event selection and reconstruction

ROOT framework [34] is used to analyze the final physics objects (such as muons and jets) provided by the simulation software. The signal and background event samples are treated in the same analysis code used to isolate the ν_4 and h candidates. The events are first tagged by the existence of at least two muons with a minimum p_T of 15 GeV. When there are more than two such muons, the two with the highest transverse momentum are considered. As the “silver mode” analysis concentrates on the hadronic decays of the W bosons originating from the heavy neutrinos, the remaining events are required to have at least 4 jets with a minimum p_T of 15 GeV on each jet. All available jets are combined

³We prefer **MadGraph** because of the ease in running it on our computational sources. With a small sample of **AlpGen**-generated events, we have validated that our results are indeed pessimistic.

⁴Both on-shell and off-shell γ and Z are considered.

Process	cross section (fb)
$W^+W^-\mu^+\mu^-$	2.56 ± 0.02
$ZZ\mu^+\mu^-$	0.70 ± 0.06
$W^+Z\mu^+\mu^-$	0.97 ± 0.01
$W^-Z\mu^+\mu^-$	0.48 ± 0.06
Direct Total	4.71 ± 0.09

Process	cross section (fb)
$\gamma \rightarrow \mu^+\mu^- W jj$	80.2 ± 1.7
$Z \rightarrow \mu^+\mu^- W jj$	630.1 ± 7.1
Total	710.3 ± 7.3
$\gamma/Z \rightarrow \mu^+\mu^- 4j$	56645.4 ± 373

Table 2: SM diboson and $2\ell + 4j$ backgrounds with corresponding cross sections. All values are MadGraph results except the $\gamma/Z \rightarrow \mu^+\mu^- 4j$ which is obtained from AlpGen.

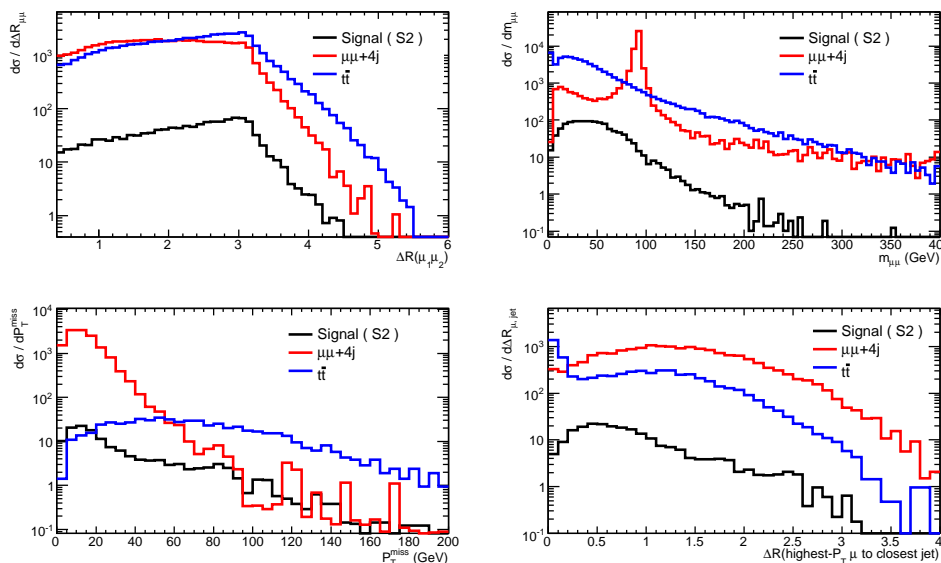


Figure 7: Kinematic distributions for the backgrounds and the signal (benchmark point $S2$). In all plots, the black solid lines represent the signal events.

to find the best two W boson candidates by taking the pair with the smallest difference from the true value of m_W [1]. A further selection is applied to restrict the reconstructed invariant masses of the dijet candidates to be within 20 GeV of the W boson mass. To reject muons from the decays of the b quarks, an isolation criterion is applied: if ΔR between a muon and the closest jet of $P_T > 20$ GeV is less than 0.4, the event is rejected. The $\Delta R_{\mu j}$ distribution for signal and two background event types are shown on the lower left side of figure 7 for the benchmark point $S2$. As the signal events do not contain any missing energy nor any b -tagged jets, these properties are used to suppress the $t\bar{t}$ background. The E_T^{miss} distribution for signal and two background event types are shown on the lower side of figure 7 for the benchmark point $S2$. The efficiencies of all the selection criteria are listed in table 3. The last row shows the common reconstruction efficiency, $\epsilon_{\text{reco}}^{\text{common}}$, the product of all individual efficiencies for all benchmark points and for the two background types.

3.4 Dirac vs Majorana neutrinos

The presented event selection and reconstruction should be extended depending on the

selection criterion	S1	S2	S3	$2\mu 4j$ background	$t\bar{t}$ background
at least 2μ	63.6	77.9	84.1	93.3	8.1
$p_T(\mu) > 15$ GeV	50.7	55.1	95.1	88.8	29.5
at least $4j$	73.6	82.3	82.6	86.0	88.7
$p_T(j) > 15$ GeV	53.3	65.6	72.2	70.4	76.0
$ m_{jj} - m_W < 20$ GeV	63.1	60.5	60.3	45.9	52.8
$\Delta R_{\mu j} > 0.4$	64.5	65.9	77.4	83.0	17.4
no j_b	93.6	92.0	91.5	93.6	53.4
$E_T^{\text{miss}} < 30$ GeV	74.4	64.9	68.7	79.4	15.4
$\epsilon_{\text{reco}}^{\text{common}}$	3.7	5.7	13.4	24.2	1.2×10^{-2}

Table 3: Selection criteria efficiencies (%) for the background and signal benchmark points. The efficiency of each criterion is listed after all the previous ones have been applied.

selection criterion	S1	S2	S3	$2\mu 4j$ background	$t\bar{t}$ background
$\text{Sign}(\mu_1) \times \text{Sign}(\mu_2) = 1$	46.6	45.5	51.2	6.8×10^{-2}	15.5
$\Delta m_{\nu_4}^{\text{reco}} / \overline{m_{\nu_4}^{\text{reco}}} < 0.25$	88.2	85.0	74.3	52.0	58.8
$\epsilon_{\text{total}}^{\text{MAJORANA}}$	1.5	2.1	5.3	8.6×10^{-3}	1.1×10^{-3}

Table 4: Efficiencies (%) of the additional selection criteria for Majorana type fourth family neutrinos.

Dirac or Majorana nature of the fourth family neutrinos. In the Dirac case, the fourth family neutrinos and their anti-particles are distinct; therefore the muons in the final state are expected to be of opposite sign. In the Majorana case, however, 50% of the time the muons in the final state is of the same sign. The following analysis deals with Dirac and Majorana cases separately.

3.4.1 Majorana case

The requirement of having same sign muons largely eliminates the SM backgrounds as seen in table 4. To further eliminate the background events, the ratio of the mass difference between the two ν_4 candidates and their average is required to be less than 0.25. Although the last requirement ensures a consistent reconstruction of both ν_4 candidates, only their average is shown in the final invariant mass histograms in figure 8 (upper row) for 1 fb^{-1} of integrated luminosity. The lower two plots in the same figure show the invariant mass distribution in the s -channel for the two benchmark points with $m_h = 300$ and $m_h = 500$ GeV. In all plots, the signal is observed to be well above the background.

3.4.2 Dirac case

The charge requirement on the muons does not reduce the background as heavily as in the Majorana case as shown in the first line of table 5. To further eliminate the background events, the di-muon invariant mass (shown on the upper right-hand of in figure 7) is required

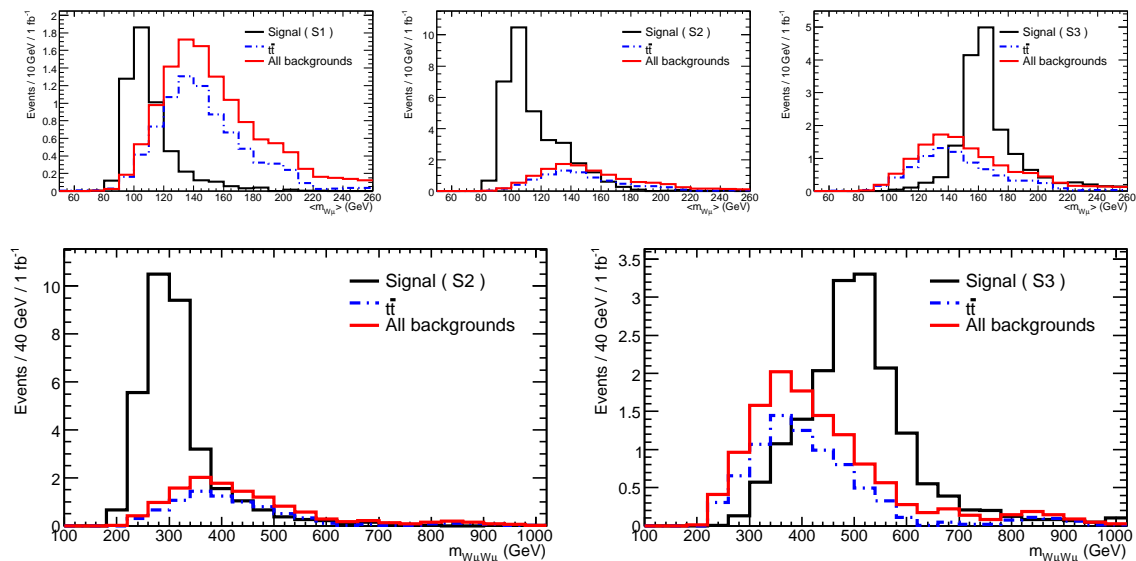


Figure 8: Majorana case: Expected event yields for the three benchmark points S1, S2 and S3 (from left to right). Histograms on the upper row show the average of the invariant masses of the two ν_4 candidates from each event, and the lower row shows the invariant masses of the reconstructed Higgs boson candidates. In all plots, the signal and background events are shown by solid black and solid gray lines, respectively. The $t\bar{t}$ component of the background is represented by the dashed histogram.

to be at least 25 GeV away from the nominal mass of the Z boson. Furthermore, to reject the muon pairs from the $\gamma_{\mu\mu}^* + 4j$ events and from the cascade decays of b quarks, an angular separation $\Delta R_{\mu\mu} > 2.0$ is required. The $\Delta R \equiv \sqrt{(\Delta\eta)^2 + (\Delta\phi)^2}$ distributions for the signal and two types of background are shown in the upper left-hand plot in figure 7.

Regardless of the considerable reduction obtained from these cuts, the $2\mu 4j$ background is still quite significant. Therefore a two dimensional selection window of $m \pm 20$ GeV is considered in the $m_{\nu_4 1}^{\text{reco}} - m_{\nu_4 2}^{\text{reco}}$ plane (figure 9). With the actual data, the centre point of this “sliding” window can be moved to search for an excess of events. For this feasibility study, the sliding selection box is centered around the true value of the ν_4 mass ($m = m_{\nu_4}^{\text{true}}$). The selection efficiency for this two dimensional selection criteria as well as the final total efficiencies for all benchmark points are listed in table 5. The invariant mass of one of the two ν_4 candidates, when the other is within the sliding window, and the reconstructed Higgs boson invariant mass, when both ν_4 candidates are in the sliding window, can be found in figure 10 in the upper and lower rows, respectively.

4. Results and discussion

The number of expected signal (s) and background (b) events are obtained by integrating the contents of the 4 bins around the signal peak for each of the histograms shown in figures 8 and 10. For the ν_4 histograms in the Dirac case, this exactly corresponds to counting the number of events in the sliding window. The statistical significance of the

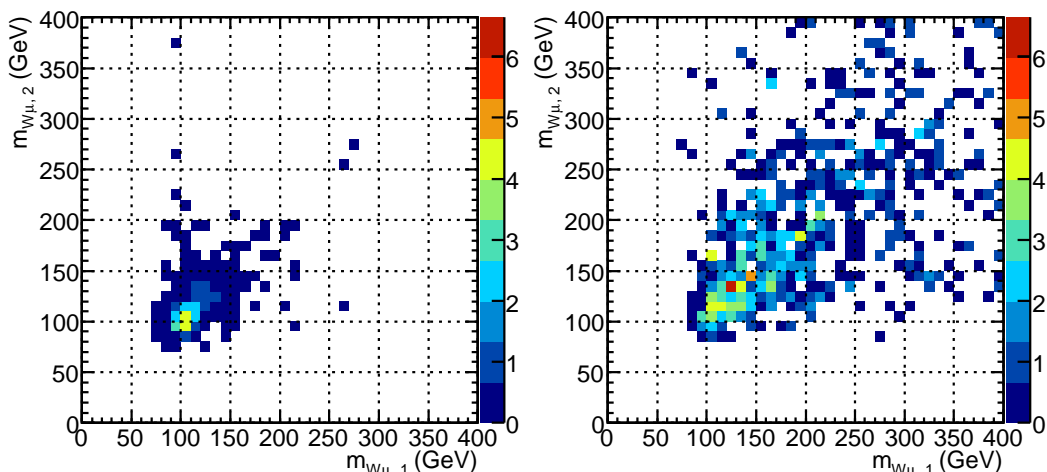


Figure 9: The invariant masses of the two reconstructed ν_4 candidates for the $S2$ signal (left) and the sum of all backgrounds (right).

selection criterion	S1	S2	$2\mu 4j$ background	$t\bar{t}$ background	S3	$2\mu 4j$ background	$t\bar{t}$ background
$\text{Sign}(\mu_1) \times \text{Sign}(\mu_2) = -1$	97.3	96.5	99.9	84.5	99.2	99.9	84.5
$ m_{\mu\mu} - m_Z > 25 \text{ GeV}$	79.1	74.1	10.0	67.7	77.6	10.0	67.7
$\Delta R_{\mu\mu} > 2.0$	72.9	65.6	34.3	59.5	74.7	34.3	59.5
$ m_{\nu_4}^{\text{reco}} - m_{\nu_4}^{\text{true}} < 20 \text{ GeV}$	67.9	60.4	5.5	6.1	39.6	6.06	13.6
$\epsilon_{\text{total}}^{\text{DIRAC}}$	1.4	1.6	4.5×10^{-2}	2.5×10^{-4}	3.1	5.0×10^{-2}	5.7×10^{-4}

Table 5: Efficiencies (%) of the additional selection criteria for Dirac type fourth family neutrinos.

expected signal was calculated using the definition: $\mathcal{S} = \sqrt{2 \times [(s + b) \ln(1 + \frac{s}{b}) - s]}$ [35]. The table 6, contains the number of signal and background events, and the significance for the three benchmark points. The signal significance as a function of the integrated luminosity is given in figure 11 for both ν_4 and h signals. For non-zero significance, a minimum of 3 signal events were required. It is seen that, depending on their masses, an early double discovery of both the Higgs boson $t\bar{t}$ and the fourth family neutrino is possible in the first year of the LHC operation, i.e., with one fb^{-1} of data. Furthermore, the integrated luminosity necessary to claim a 3σ observation and a 5σ discovery is given in table 7 for all the considered scenarios.

5. Conclusions

While hadron colliders are not considered to be the best place to search for heavy charged and neutral leptons due to small production cross section, the existence of the Higgs particle might drastically change this picture. For example, if the Higgs mechanism is the one that Nature chose to give masses to the fermions, the LHC has the chance to simultaneously discover both the Higgs boson itself and the fourth family neutrino using the $pp \rightarrow h \rightarrow \nu_4 \bar{\nu}_4$ channel. The main reason for this possibility is the enhancement of the gluon fusion process due to fourth family quarks yielding a high Higgs boson production rate. If $m_h = 300 \text{ GeV}$

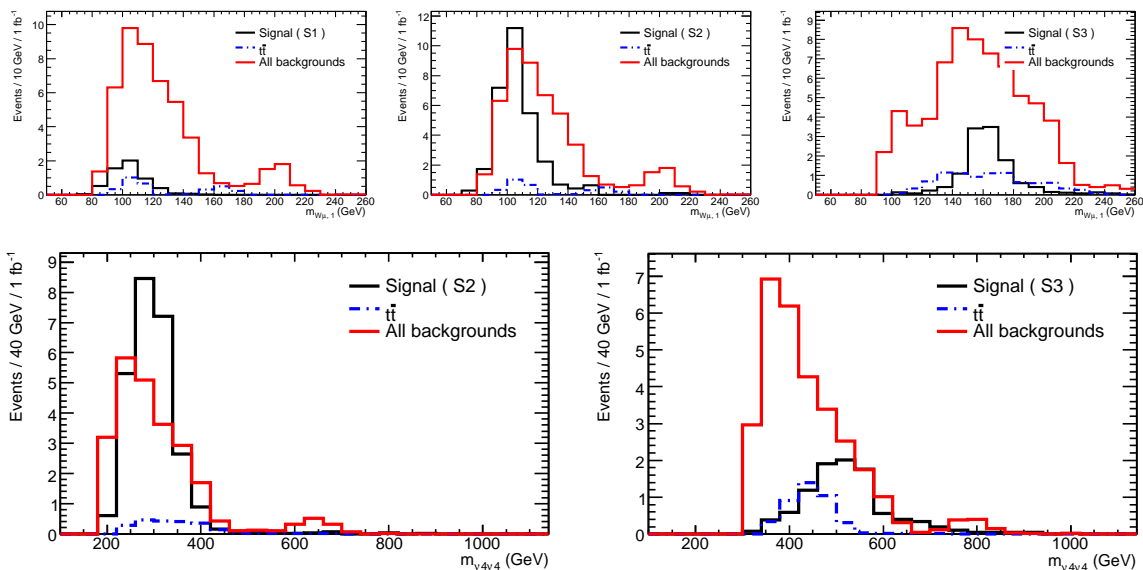


Figure 10: Dirac case: Expected event yields for the three benchmark points S1, S2 and S3 (from left to right). Histograms on the upper row show the invariant mass of one of the two ν_4 candidates from each event, when the other candidate is required to be within 20 GeV of the true mass. The lower row shows the invariant masses of the reconstructed Higgs boson candidates when both ν_4 candidates satisfy the sliding window cuts. In all plots, the signal and background events are shown by solid black and solid gray lines, respectively. The $t\bar{t}$ component of the background is represented by the dashed histogram.

Benchmark Point	ν_4			h		
	signal	backgrd	significance	signal	backgrd	significance
$S1_{\text{Dirac}}$	5.1	26.3	1.0	N/A	N/A	N/A
$S2_{\text{Dirac}}$	25.6	26.3	4.4	23.6	17.5	4.8
$S3_{\text{Dirac}}$	9.8	30.5	1.7	6.9	11.9	1.8
$S1_{\text{Majorana}}$	4.2	1.4	2.7	N/A	N/A	N/A
$S2_{\text{Majorana}}$	23.2	1.4	9.7	28.7	5.0	8.4
$S3_{\text{Majorana}}$	12.4	4.7	4.4	10.6	4.0	4.1

Table 6: For the three benchmark points, the statistical significance for the discovery of the heavy neutrino ν_4 and of the Higgs boson estimated at 1fb^{-1} of integrated luminosity.

Benchmark Point	ν_4		h	
	Dirac	Majorana	Dirac	Majorana
$S1$	9800 (27000)	1300 (3500)	N/A	N/A
$S2$	470 (1300)	100 (270)	390 (1100)	130 (350)
$S3$	3200 (8800)	470 (1300)	2700 (7400)	540 (1500)

Table 7: Required integrated luminosity in pb^{-1} for 3 (5) σ statistical significance for the discovery of the heavy neutrino ν_4 and of the Higgs boson, for the three benchmark points.

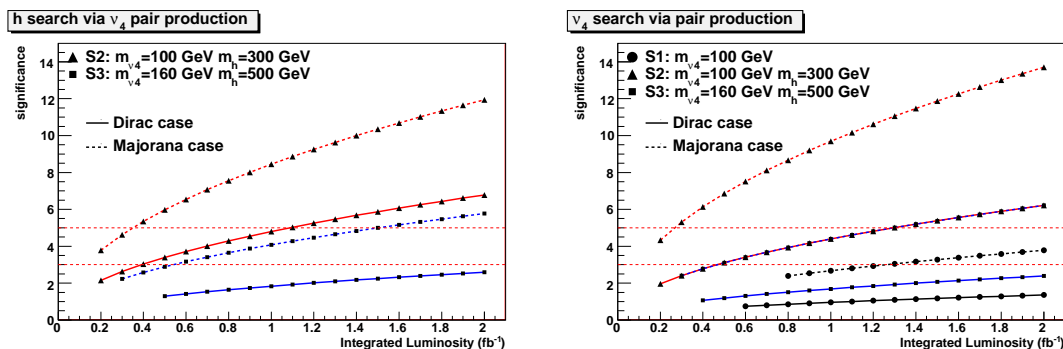


Figure 11: Expected signal significance for the Higgs boson and fourth family neutrino searches. For each point on the curves, at least 3 signal events are required to have satisfied all the selection criteria.

and $m_{\nu_4} = 100$ GeV, LHC would discover both of them with 5σ significance even with an integrated luminosity of around 350 pb^{-1} , provided the fourth family neutrinos are of Majorana nature. Alternatively, if they are of Dirac nature, the double discovery of ν_4 and h is again possible with less than 1.5 fb^{-1} of data. For heavier particles ($m_h = 500$ GeV and $m_{\nu_4} = 160$ GeV), the signals from Majorana (Dirac) type neutrinos and the Higgs boson can also be observed with about 1.5 (9) fb^{-1} of data. A similar result has been obtained for another process ($pp \rightarrow W^+ \rightarrow \ell^+ N \rightarrow \ell^+ \ell^+ jj$) in a recent paper [36].

Finally, if the Higgs boson does not exist, the Z boson provides the only tree-level channel for the pair production of fourth family neutrinos. This study shows that the 5σ significance can be attained with about 3.5 fb^{-1} for the Majorana type and about 30 fb^{-1} for Dirac type neutrinos. However, a more detailed search, also involving the semi-leptonic di- W boson decays would reduce the amount of data-taking time needed. Such a study is in progress.

Acknowledgments

The authors would like thank Paul Coe and Jeff Tseng for useful suggestions. S.S. acknowledges the support from the Turkish State Planning Committee under the contract DPT2006K-120470 and from the Turkish Atomic Energy Authority (TAEK). G.Ü.'s work is supported in part by U.S. Department of Energy Grant DE FG0291ER40679. M.K.Ü., T.C.D. and V.E.Ö. acknowledge support from the UK Science and Technology Facilities Council (STFC).

References

- [1] PARTICLE DATA GROUP collaboration, W.M. Yao et al., *Review of particle physics*, *J. Phys.* **G 33** (2006) 1.
- [2] H.-J. He, N. Polonsky and S.-f. Su, *Extra families, Higgs spectrum and oblique corrections*, *Phys. Rev. D* **64** (2001) 053004 [[hep-ph/0102144](#)].

- [3] V.A. Novikov, L.B. Okun, A.N. Rozanov and M.I. Vysotsky, *Extra generations and discrepancies of electroweak precision data*, *Phys. Lett.* **B 529** (2002) 111 [[hep-ph/0111028](#)].
- [4] G.D. Kribs, T. Plehn, M. Spannowsky and T.M.P. Tait, *Four generations and Higgs physics*, *Phys. Rev.* **D 76** (2007) 075016 [[arXiv:0706.3718](#)].
- [5] H. Fritzsch, *Light neutrinos, nonuniversality of the leptonic weak interaction and a fourth massive generation*, *Phys. Lett.* **B 289** (1992) 92.
- [6] A. Datta, *Flavor democracy calls for the fourth generation*, *Pramana* **40** (1993) L503 [[hep-ph/9207248](#)].
- [7] A. Celikel, A.K. Ciftci and S. Sultansoy, *A search for fourth SM family*, *Phys. Lett.* **B 342** (1995) 257.
- [8] A. Datta and S. Raychaudhuri, *Quark masses and mixing angles in a four generation model with a naturally heavy neutrino*, *Phys. Rev.* **D 49** (1994) 4762.
- [9] S. Atag et al., *The fourth SM family, breaking of mass democracy and the CKM mixings*, *Phys. Rev.* **D 54** (1996) 5745.
- [10] A.K. Ciftci, R. Ciftci and S. Sultansoy, *The fourth SM family neutrino at future linear colliders*, *Phys. Rev.* **D 72** (2005) 053006 [[hep-ph/0505120](#)].
- [11] S. Sultansoy, *Flavor democracy in particle physics*, *AIP Conf. Proc.* **899** (2007) 49 [[hep-ph/0610279](#)].
- [12] G. Bregar, M. Breskvar, D. Lukman and N.S. Mankoc Borstnik, *On the origin of families of quarks and leptons-predictions for four families*, *New J. Phys.* **10** (2008) 093002 [[arXiv:0708.2846](#)].
- [13] W.-S. Hou, M. Nagashima, G. Raz and A. Soddu, *Four generation CP-violation in $B \rightarrow \phi K^0, \pi^0 K^0, \eta' K^0$ and hadronic uncertainties*, *JHEP* **09** (2006) 012 [[hep-ph/0603097](#)].
- [14] W.-S. Hou, M. Nagashima and A. Soddu, *Large time-dependent CP-violation in B_s^0 system and finite D^0 - \bar{D}^0 mass difference in four generation standard mode*, *Phys. Rev.* **D 76** (2007) 016004 [[hep-ph/0610385](#)].
- [15] A. Soni, A.K. Alok, A. Giri, R. Mohanta and S. Nandi, *The fourth family: a natural explanation for the observed pattern of anomalies in B-CP asymmetries*, [arXiv:0807.1971](#).
- [16] ATLAS collaboration, *ATLAS detector and physics performance technical design report*, CERN-LHCC-99-14/15 (1999), see section 18.2.
- [17] E. Arik et al., *Search for the fourth family up quarks at CERN LHC*, *Phys. Rev.* **D 58** (1998) 117701.
- [18] B. Holdom, *The discovery of the fourth family at the LHC: what if?*, *JHEP* **08** (2006) 076 [[hep-ph/0606146](#)]; *t' at the LHC: the physics of discovery*, *JHEP* **03** (2007) 063 [[hep-ph/0702037](#)]; *The heavy quark search at the LHC*, *JHEP* **08** (2007) 069 [[arXiv:0705.1736](#)].
- [19] V.E. Özcan, S. Sultansoy and G. Ünel, *Search for 4th family quarks with the ATLAS detector*, [arXiv:0802.2621](#).
- [20] S. Sultansoy and G. Unel, *'Silver' mode for the heavy Higgs search in the presence of a fourth SM family*, [arXiv:0707.3266](#).

- [21] CDF collaboration, *Search for heavy top $t\bar{t} \rightarrow Wq$ in lepton plus jet events*, CDF Conference Note 8495 (2007).
- [22] E. Arik, O. Cakir, S.A. Cetin and S. Sultansoy, *Consequences of the extra SM families on the Higgs boson production at Tevatron and LHC*, *Phys. Rev. D* **66** (2002) 033003 [[hep-ph/0203257](#)];
E. Arik et al., *Can the Higgs boson be discovered at the LHC with integrated luMINOSity of order fb^{-1} ?*, *Eur. Phys. J. C* **26** (2002) 9 [[hep-ph/0109037](#)];
E. Arik, O. Cakir, S.A. Cetin and S. Sultansoy, *Observability of the Higgs boson and extra SM families at the Tevatron*, *Acta Phys. Polon.* **B37** (2006) 2839 [[hep-ph/0502050](#)].
- [23] U. Langenegger, M. Spira, A. Starodumov and P. Trub, *SM and MSSM Higgs boson production: spectra at large transverse momentum*, *JHEP* **06** (2006) 035 [[hep-ph/0604156](#)].
- [24] M.S. Chanowitz, *A Z' boson and the Higgs boson mass*, [arXiv:0806.0890](#).
- [25] D. Choudhury, R.M. Godbole and P. Roy, *Higgs mediated heavy neutrino pair production at pp supercolliders*, *Phys. Lett. B* **308** (1993) 394 [*Erratum ibid.* **314** (1993) 482] [[hep-ph/9211240](#)].
- [26] A. Pukhov, *CalcHEP 3.2: mSSM, structure functions, event generation, batchs and generation of matrix elements for other packages*, [hep-ph/0412191](#);
COMPHEP collaboration, E. Boos et al., *CompHEP 4.4: automatic computations from lagrangians to events*, *Nucl. Instrum. Meth.* **A534** (2004) 250 [[hep-ph/0403113](#)].
- [27] J. Alwall et al., *MadGraph/MadEvent v4: the new web generation*, *JHEP* **09** (2007) 028 [[arXiv:0706.2334](#)].
- [28] R. Mehdiyev, S. Sultansoy, G. Unel and M. Yilmaz, *Search for E_6 isosinglet quarks in ATLAS*, *Eur. Phys. J. C* **49** (2007) 613 [[hep-ex/0603005](#)].
- [29] T. Sjöstrand et al., *High-energy-physics event generation with PYTHIA 6.1*, *Comput. Phys. Commun.* **135** (2001) 238 [[hep-ph/0010017](#)].
- [30] M.L. Mangano, M. Moretti, F. Piccinini, R. Pittau and A.D. Polosa, *ALPGEN, a generator for hard multiparton processes in hadronic collisions*, *JHEP* **07** (2003) 001 [[hep-ph/0206293](#)].
- [31] J. Conway, *PGS 4: Pretty Good Simulation of high energy collisions*, <http://www.physics.ucdavis.edu/~conway/research/software/pgs/pgs4-general.htm> (2006).
- [32] ATLAS collaboration, *Expected performance of the ATLAS experiment, detector, trigger and physics*, CERN-OPEN-2008-020 (2008), to appear.
- [33] J. Pumplin et al., *New generation of parton distributions with uncertainties from global QCD analysis*, *JHEP* **07** (2002) 012 [[hep-ph/0201195](#)].
- [34] THE ROOT TEAM, *ROOT 5.18.00, an object-oriented data analysis framework*, <http://root.cern.ch>;
J. Alwall et al, *ExRootAnalysis 1.0.6*, *JHEP* **09** (2007) 028 [[arXiv:0706.2334](#)].
- [35] CMS collaboration, *CMS physics, technical design report*, CERN-LHCC-2006-001.
- [36] F. del Aguila, J.A. Aguilar-Saavedra and R. Pittau, *Heavy neutrino signals at large hadron colliders*, *JHEP* **10** (2007) 047 [[hep-ph/0703261](#)].